Emittance preservation of an electron beam in a loaded quasi-linear plasma wakefield

Veronica K. Berglyd Olsen* and Erik Adli
University of Oslo, Oslo, Norway

Patric Muggli
Max Planck Institute for Physics, Munich, Germany and CERN, Geneva, Switzerland

(Dated: September 29, 2017)

We investigate beam loading and emittance preservation for a high-charge electron beam being accelerated in quasi-linear plasma wakefield driven by a short proton beam. The structure of the wakefield is similar to that of a long, modulated proton beam, such as the one being studied by AWAKE. We show that by exploiting two well known effects, full blow out of plasma electrons by the accelerated beam, and beam loading of the wake field, the electron beam can be accelerated without significant emittance growth.

I. INTRODUCTION

Beam driven plasma wakefield accelerators have the potential to offer compact linear accelerators with high energy gradients, and have been of interest for several decades [1]. With a relativistic charged particle drive beam travelling through a plasma, a strong wakefield is excited, that can be loaded by a trailing witness beam. When the witness beam optimally loads the wakefield, an increase in absolute energy spread can be kept to a minimum. The concept has been demonstrated experimentally in the past using electron drive beams accelerating electron witness beams [2–4]. AWAKE at CERN is a proof of concept beam driven plasma wakefield accelerator experiment using a proton drive beam delivered by the SPS accelerator [5].

A major challenge with plasma wakefield accelerators is, however, to accelerate a beam while keeping energy spread and emittance growth to a minimum. In the well described linear case where the beam density n_b is much smaller than the plasma density n_0, a non-linear transverse focusing force causes emittance growth of the witness beam. the beam will also see a transversely and longitudinally varying accelerating field causing a spread in energy after the beam has been accelerated [6]. In the non-linear regime, where $n_b > n_0$, a bubble is formed by the transverse oscillations of the plasma electrons, forming a sheet around an evacuated area filled with only ions. The ions, assumed stationary, form an uniform density ion channel creating a focusing force that varies linearly with radius. This produces a focusing force that preserves emittance [7, 8].

In this paper we present simulation results showing how we can use the non-linear wakefields driven by the head of a high charge density witness beam to reduce energy spread and emittance growth in the rest of the beam, while being accelerated by a proton drive beam producing quasi-linear wakefields.

* v.k.b.olsen@cern.ch

A. Self-modulation as a Driver

A train of electron drive bunches with a separation λ_{pe} and a length $l_b \ll \lambda_{pe}$, where the plasma wavelength $\lambda_{pe} = 2\pi c/\omega_{pe}$ and the plasma frequency $\omega_{pe} = (n_0 e^2/m_e \epsilon_0)^{1/2}$, produces a field E_z that increases for each drive bunch [1]. A tailing witness beam loading the peak accelerating phase of this field will gain energy from the wakefield from all of the drive bunches when they are properly phased with respect to the wakefields. Acceleration of an electron witness beam driven by two electron drive beams has been demonstrated at Brookhaven National Laboratory [9].

The energy carried by electron drive bunches used in previous experiments were typically small – on the order of 100 J – and the propagation length typically < 1 m [3, 10]. Higher energy electron beam can be improve the propagation length and thus the energy of the accelerated beam. For instance, the energy of a high-charge electron beam accelerated to 1 TeV, similar to the beam that could be produced by the international linear collider with 1×10^{10} electrons, is 1.6 kJ. By using electron beams or lasers pulses as drivers, a large number of plasma stages is required. However, staging plasma accelerators without reducing the effective gradient and spoiling the beam quality is challenging [11, 12].

Proton beams available at CERN carry significantly more energy, 19 kJ for the SPS beam [13], allowing for much longer plasma wakefield accelerator stages. The SPS beam is, unfortunately, orders of magnitude longer than the plasma wavelengths needed for such applications. This can be resolved by letting the proton beam undergo self-modulation before injecting the witness beam into accelerating structure. The self-modulation of the beam is produced by the transverse fields generated by the beam acting upon itself, causing regions of the beam to rapidly defocus [14]. The modulation frequency is close to that of the plasma, and produces a train of short proton bunches along the beam axis with a surrounding halo of defocused particles. This train of bunches resonantly produces wakefields to larger ampli-

tudes.

B. AWAKE Run 2

The AWAKE experiment, currently in its first stages of operation at CERN, uses a 400 GeV beam delivered by the SPS as its driver, and a single 10 m plasma stage with a nominal plasma density of $7\times10^{14}\,\mathrm{cm}^{-3}$ [13]. This plasma density corresponds to $\lambda_{pe} = 1.26\,\mathrm{mm}$ – matched to the transverse size of the SPS proton beam such that $k_{pe}\sigma_{x,y} = 1$, where $k_{pe} = 2\pi/\lambda_{pe}$ is the plasma wave number.

The aim of the first phase of Run 1 of the experiment is to demonstrate self-modulation of the proton beam. The aim of the second phase in 2018 is to sample the wakefield with a long electron beam $\simeq \lambda_{pe}$. The study presented here is for Run 2 [15], which aims to demonstrate acceleration of a short electron beam, $\ll \lambda_{pe}$, to high energy with a minimal increase in emittance and absolute energy spread.

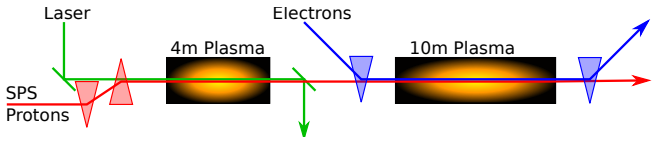

FIG. 1. A simplified illustration of the experimental setup for AWAKE Run 2. The SPS proton beam undergoes self-modulation in the first plasma section. The electron witness beam is injected into the accelerating structure, and undergoes acceleration in the second plasma stage [15, 16].

The plans for AWAKE Run 2 proposes to use two plasma sections, illustrated in figure 1. The first section of 4 m is the self-modulation stage where the proton beam undergoes self-modulation without the electron beam present. The electron witness beam is then injected into the modulated proton beam before stage two, where it undergoes acceleration.

Using the SPS proton beam as driver, the self-modulated proton beam does not produce a full non-linear wakefield, and not all plasma electrons are therefore evacuated from the plasma bubble. The result is that the focusing force does not increase linearly with radius. The small size of the accelerating structure produced by the self-modulated beam also puts constraints on the size of the electron witness beam, and thus its charge and current, if at the same time we wish to prevent large energy spread. By matching the transverse size of the beam at a given emittance to the plasma density, we prevent large amplitude oscillations which may cause additional energy spread as well as emittance growth.

The key idea is to have enough charge in the witness beam to at the same time load the wakefield to produce low relative energy spread $\Delta E/E$, and blow out the electrons left in the accelerating structure to reach conditions that preserves emittance.

II. METHOD

A main focus of this study is on the loading of the wakefields driven by the proton beam. In order to eliminate other factors that may affect this, like decay and defocusing of the proton beam, we tried several approaches to create a stable drive beam structure based in previous self-modulation studies.

In these studies we used a short, pre-modulated proton beam with similar structure to the beam produced by the self-modulation of the SPS beam in AWAKE. These studies were done using the full PIC code Osiris [17] using 2D cylindrical-symmetric simulations and primarily looked at beam loading, energy gain and energy spread [16, 18].

In order to study the witness beam emittance evolution we turned to the recently released open source version of QuickPIC. QuickPIC is a fully relativistic 3D quasi-static PIC code [19, 20]. It does not suffer from the numerical Cherenkov effect that full PIC codes do [21, 22], making it a well suited tool to study emittance preservation.

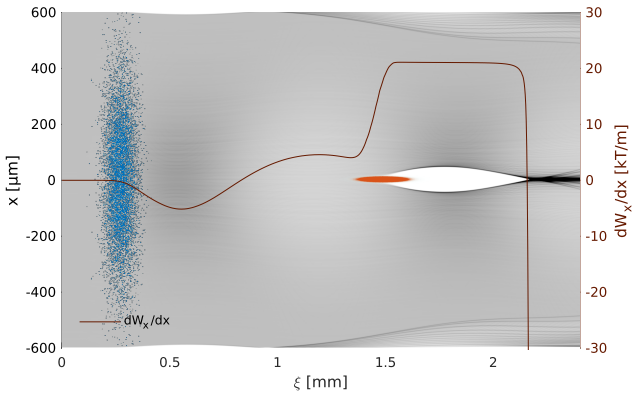

FIG. 2. The plasma density in grey with the drive beam (blue) and the witness beam (red) superimposed. The line plot indicates the transverse wakefield gradient dW_x/dx where $W_x = E_x - v_b B_y$, evaluated along the beam axis.

A. Drive Beam Parameters

The baseline AWAKE drive beam current is insufficient to reach the non-linear regime and produce a plasma bubble. When the SPS beam, containing 3×10^{11} protons [13], enters the second plasma stage, the peak electric field is expected to be $500-600\,\mathrm{MV/m}$. The plasma electrons are only depleted to around 65% of nominal plasma density at the point where we inject the electron beam [23]. In our simulation these conditions are replicated using a single proton beam of 1.46×10^{10} protons, or 2.34 nC and 7 kA.

The peak density of the simulation drive beam is $0.83\cdot n_0$, producing a quasi-linear wakefield. The single bunch setup uses the baseline proton beam energy of

400 GeV and transverse size $\sigma_x = 200\,\mu$m. We also set the length of the drive beam to $\sigma_z = 40\,\mu$m. We are not considering the evolution of the proton beam itself in this study, so in order to create a stable environment to study the evolution of the witness beam we prevent the proton beam from evolving radially by increasing the particle mass by 6 orders of magnitude.

B. Witness Beam Parameters

Beam loading of a short witness beam is sensitive to its position relative to the electric field [24]. A low gamma witness beam can easily drift out of phase with the drive beam wakefield. The drift of the beams is proportional to γ^{-2}, so to eliminate initial de-phasing of the witness beam, initial beam energy was set such that $\gamma_{eb} = \gamma_{pb} = 426.3$, giving an energy of 217 MeV. A lower initial value is likely to be sufficient [16].

In these simulations we have used a matched beam for an initial normalised emittance of $\epsilon_N = 2\,\mu$m. The beam matching relation is given by

$$\beta = \frac{\sigma_{x,y}^2 \gamma}{\epsilon_N} = \frac{c}{\omega_{pe}}\sqrt{2\gamma}, \tag{1}$$

where β is the Twiss parameter. It then follows that the transverse profile of the beam must satisfy

$$\sigma_{x,y}^2 = c\epsilon_N \sqrt{2\frac{m_e \varepsilon_0}{n_{pe} e^2 \gamma}} \tag{2}$$

in order to be matched to a given plasma density, initial emittance and energy. This relation requires a very narrow beam with a $\sigma_{x,y}$ of 5.25 μm compared to the drive beam $\sigma_{x,y} = 200\,\mu$m. The charge density of this compact witness beam reaches that of the plasma density at only a few pC, but reaches optimal beam loading at around $100 - 200$ pC. The implication here being that the witness beam produces its own non-linear wakefield already at the head of the beam. The majority of the electrons within it will therefore see a linear focusing force preventing the bulk of the beam from undergoing emittance growth.

The relatively small size of the witness beam compared to the proton beam put some restrictions on the transverse resolution of the witness beam as we need a simulation box wide enough to contain the larger beam while resolving the narrower one (see figure 2). We used a transverse grid cell size of 1.17 μm, and of 2.34 μm for the longitudinal grid cells for the simulations presented in section III. The witness beam was simulated with 16.8×10^6 non-weighted particles. The witness beam has a total charge of 100 pC, a $\sigma_z = 60\,\mu$m, and a $\sigma_x = 5.25\,\mu$m matching an initial normalised emittance $\epsilon_0 = 2\,\mu$m. We refer to this parameter set as our base case.

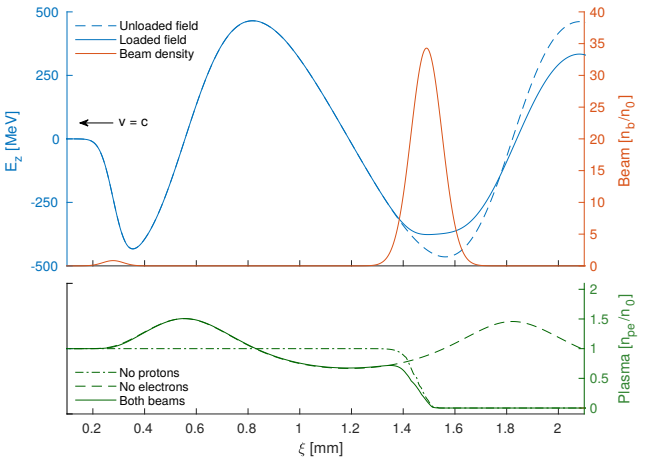

FIG. 3. The top plot shows the unloaded longitudinal electric field with no witness beam (dashed blue line) and the loaded field (whole blue line) along the beam axis. The beam density along the axis for both beams are shown in red. The bottom plot compares the plasma densities along the beam axis for a drive beam with no witness beam (dashed green line), witness beam with no drive beam (dash-dotted green line), and both beams present (whole green line). $\xi = z - tc$ is the position in the simulation box, moving towards the left.

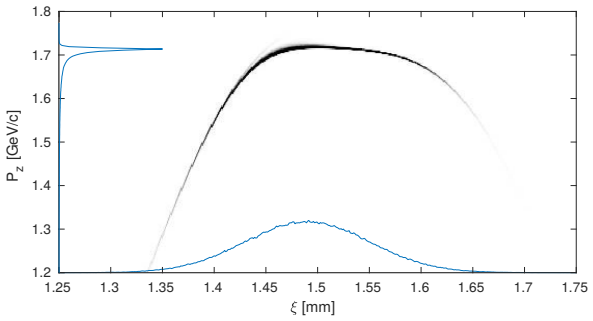

FIG. 4. The phase space charge distribution of a 100 pC, 60 μm long witness beam after 4 m of plasma. The mean momentum is 1.67 GeV/c with an RMS energy spread of 87 MeV/c (5.2%) for the full beam.

III. BEAM LOADING

The single drive beam setup is designed to produce similar initial conditions for the witness beam as the self-modulated case. However, since the drive beam is prevented from significant transverse evolution, we are presented with an idealised case where the electron witness beam sees consistent wakefields throughout the plasma stage. The E_z-field generated by the proton drive beam is seen as the blue line in figure 3, shown with and without the electron beam present. With a proton beam density $n_{pb} \simeq n_0$, we are in the quasi-linear regime [25]. The dashed green line in the lower part of figure 3 shows that the on-axis plasma density has a depletion of 67%,

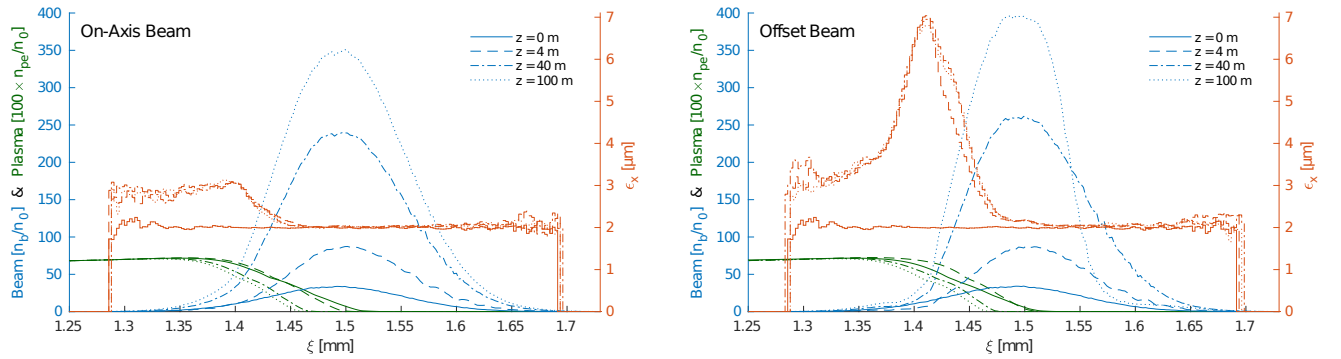

FIG. 5. Beam density in blue along the beam axis for an on-axis beam with respect to the drive beam axis (left), and an offset beam (right) with an offset of one $\sigma_x = 5.24\,\mu$m in the x-plane. At four different positions z in the plasma stage. The red lines show a moving window calculation of transverse normalised emittance. The moving window calculation uses longitudinal slices of $l = 4 \times \Delta\xi = 9.38\,\mu$m with a step of $\Delta\xi$. Only slices with more than 100 macro particles have been included. The plasma density profile is included in green, and scaled up by a factor of 100 to be visible. These simulations were run with an LHC energy drive beam of 7 TeV

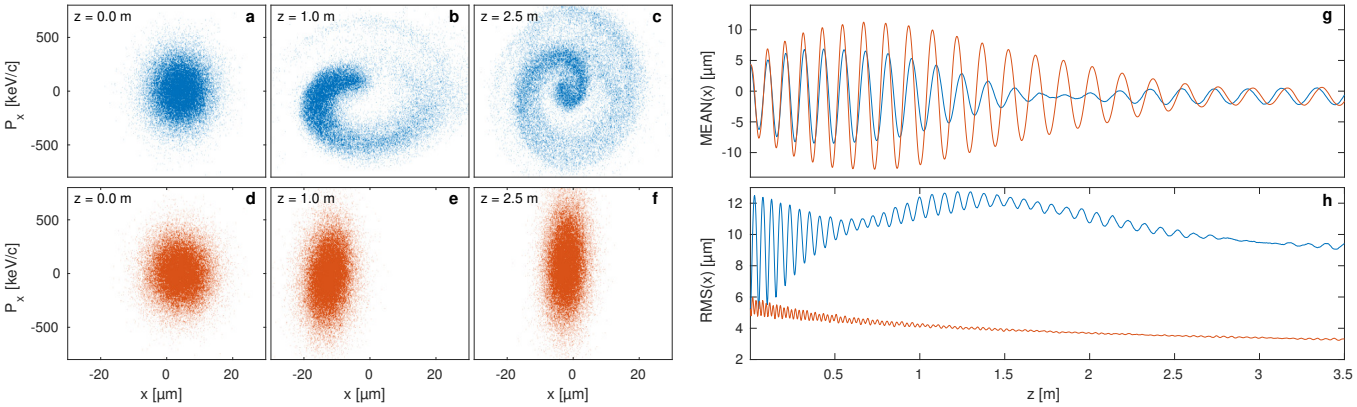

FIG. 6. Plots **a** to **f** show the transverse phase space of the offset electron beam at different plasma positions. Plot **g** shows the macro particle mean position, and plot **h** their RMS spread. Plots **a**, **b** and **c**, as well as the blue lines in plots **g** and **h** represent particles with position $1.40\,\mu\text{m} < \xi < 1.42\,\mu$m. Plots **d**, **e** and **f**, and the red lines in plots **g** and **h** represent particles with position $1.55\,\mu\text{m} < \xi < 1.57\,\mu$m.

close to what we see in full scale reference simulations for AWAKE Run 2 [23].

The witness beam generates its own wakefield which partially cancels out the E_z field generated by the drive beam. With an ideally shaped electron beam charge profile it is possible to optimally load the field in such a way that the accelerating field is constant along the beam [6, 24]. However, a Gaussian beam cannot completely flatten the electric field and thus accelerate the beam with no spread in energy. Our base case beam has a tail in energy both at the front and the back of the beam, as illustrated in figure 4, but the bulk of the sees a relatively flat field when $n_{eb} \approx 35 \times n_0$. This means that the witness beam's own wakefield is in the fully non-linear regime, where the space charge force is sufficient to blow-out all plasma electrons resulting in the formation of an ion column. This ion column, as is well known [26], provides a linear focusing force on the part the electron beam within the column, and therefore prevents emittance growth for this region of the beam. This effect is shown for our base case in figure 2. The focusing field has a gradient of 20 kT/m near the beam axis. However, with such a narrow beem wehn matched beam to the plasma density (equation 1), we are limited on how much total charge we can accelerate without reaching charge densities that will overload the field.

For the majority of the cases we studied, that maintained a stable accelerating structure, about $70 - 80\%$ of the electron beam retained its initial emittance. Figure 5 shows emittance along the beam for the base case, sampled after propagating through 0, 4, 40 and 100 m of plasma. Emittance growth mainly occurs in first few meteres, and no significant emittance growth was observed after this for propagation lengths up to 100 m. For this simulation, drive beam energy was increased to 7 TeV (LHC energy) to prevent de-phasing, as de-phasing

starts to become a significant effect for the SPS beam of 400 GeV after about 50 m.

Since the accelerated electron beam creates its own plasma bubble, the emittance of the part of the beam inside the bubble is not affected by small beam offsets with respect to the proton beam axis. This is an added benefit of this new accelerating regime, and may ease the transverse injection tolerances. The head of the beam does not benefit from this effect, but since the proton beam creates a quasi-linear wake, the head of the beam still stabilises after some time. This is illustrated in figure 5 for an electron beam offset of $1\sigma_x$. In this case there is a larger initial emittance growth (see figure 6a-f), but the emittance growth stops after the first few metres (figure 5). This effect is likely to be greater for larger offsets as the beam oscillates around the axis of the drive beam wakefield, as can bee seen from in figure 6g-h.

The transverse beam size within the bubble, where normalised emittance is preserved, follows the evolution given by equation 2 where the plasma density is given by the ion density. The on-axis density of the electron beam, as a result, increases as its gamma factor increases and its transverse size decreases. The effect can be seen in figure 6h. This has the potential to cause overloading of the field. However, for our base case this effect was not significant.

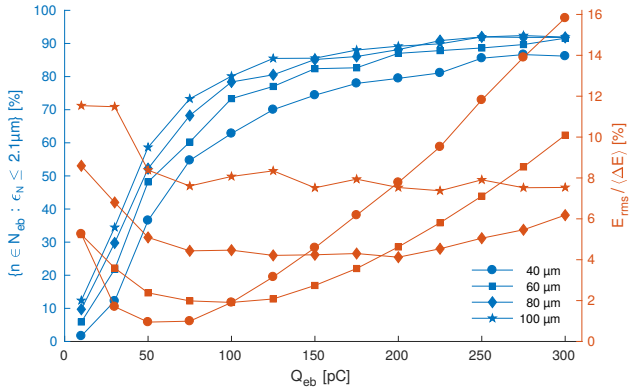

FIG. 7. Ratio of total beam charge with an emittance growth $\Delta\epsilon \leq 5\%$ as a function of initial beam charge (blue), and relative energy spread of the accepted charge (red), after 4 m of plasma and with an initial emittance $\epsilon_{N,0} = 2\,\mu$m. These are shown for four different σ_z from 40 μm to 100 μm. The detailed studies presented in beam loading section corrspond to the square marked lines at 100 pC.

IV. PARAMETER OPTIMISATION

The beam loading and blow out properties of the electron beam depends on a large number of parameters, including the longitudinal profile, the transverse profile as well as the relative phasing of the proton and the electron beams.

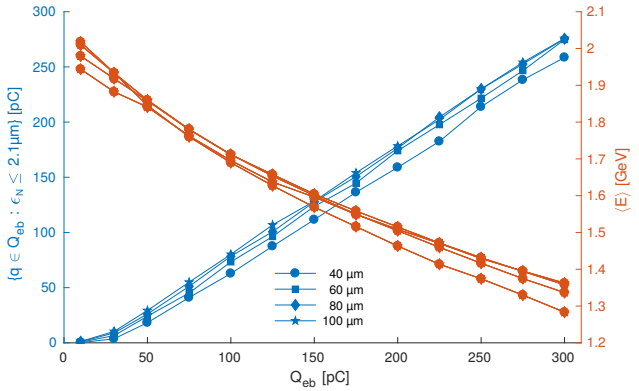

FIG. 8. Total beam charge with an emittance growth $\Delta\epsilon \leq 5\%$ as a function of initial beam charge (blue), and final momentum (red), after 4 m of plasma and with an initial emittance $\epsilon_{N,0} = 2\,\mu$m.

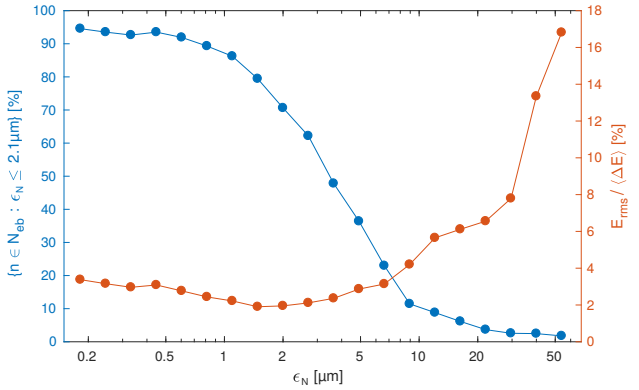

FIG. 9. Ratio of total beam charge with an emittance growth $\Delta\epsilon \leq 5\%$ as a function of initial emittance (blue), and relative energy spread of the accepted charge (red), after 4 m of plasma.

For AWAKE Run 2 we desire to maximize the energy gain, minimize the energy spread, maximize the charge to be accelerated, and minimize the emittance growth. In addition, the bunch length should be such that it is possible to generate and transport by a compact electron injector [15]. These are contradictory constraints. We investigate the interdependence of these parameters in our simulation by varying the electron bunch length, its charge, and initial emittance. The results were quantified in terms of how much of the initial charge retained its initial emittance within a 5% margin. For these parameter scans we used a transverse grid cell size of 2.34 μm, and let the beams proagate through 4 m of plasma.

Figures 7 and 8 show the dependence on bunch length and bunch charge for an initial beam emittance of 2 μm. We ran the scan with beam charges from 10 pC to 300 pC and with length σ_z from 40 μm to 100 μm. As can be seen from figure 7, both the 40 μm and the 60 μm beam has a well defined minimum energy spread with a beam charge

$\approx 50\,\mathrm{pC}$ and $\approx 100\,\mathrm{pC}$ respectively. Lower beam charges tend to underload the electric field, while higher beam charges tend to overload it. It is also clear that longer beams with respect to the accelerating phase of the field, $\approx \lambda_{pe}/4$, will not optimally load the, thus producing a larger spread in energy.

Figure 9 shows how the growth in emittance and energy spread varies with initial electron beam emittance. The smaller the initial emittance is, the better the emittance is preserved. There are two effects that lead to growth for high emittance beams; the transverse beam size may increase beyond the size of the bubble, or the beam density may be reduced so much that the plasma electrons are no longer fully evacuated from the ion column. Emittance values higher than a few micrometres lead to a significant increase in both emittance and energy spread. In these simulations the focusing of the beam to the plasma remains matched for each emittance value.

V. CONCLUSION

We have studied a new plasma wakefield acceleration regime; acceleration of a strongly loaded electron beam in a quasi- linear proton driven wake. When optimally loaded, the electron beam creates its own ion bubble, yielding emittance preservation for a large parts of the electron beam.

These result indicates that emittance preservation for an on-axis injected electron beam, properly optimized, is feasible. Parameter studies indicate that up to a few $100\,\mathrm{pC}$ might be accelerated, for bunches of length $40 - 60\,\mu\mathrm{m}$. Such an electron bunch may be generated by a standard S-band RF gun.

As this study assumes a wake driven by a single, short proton beam, the studies for interesting cases for AWAKE should be repeated by a full simulation of a self-modulated proton beam.

VI. ACKNOWLEDGEMENTS

The simulations for this study have been run using the open source version of QuickPIC released in early 2017 and owned by UCLA.

These numerical simulations have been made possible through access to the Abel computing cluster in Oslo, Norway. Abel is maintained by UNINETT Sigma2 AS and financed by the Research Council of Norway, the University of Bergen, the University of Oslo, the University of Troms and the Norwegian University of Science and Technology. Project code: nn9303k. Some of the simulations were also run on the student-maintained computing cluster "Smaug" at the University of Oslo, Department of Physics.

The authors would also like to thank the OSIRIS Consortium for providing access to the OSIRIS framework. OSIRIS was used extensively for simulations leading to the work presented in this paper.

[1] P. Chen, J. M. Dawson, R. W. Huff, and T. Katsouleas, Physical Review Letters **54**, 693 (1985).
[2] J. B. Rosenzweig, D. B. Cline, B. Cole, H. Figueroa, W. Gai, R. Konecny, J. Norem, P. Schoessow, and J. Simpson, Physical Review Letters **61**, 98 (1988).
[3] I. Blumenfeld, C. E. Clayton, F.-J. Decker, M. J. Hogan, C. Huang, R. Ischebeck, R. Iverson, C. Joshi, T. Katsouleas, N. Kirby, W. Lu, K. A. Marsh, W. B. Mori, P. Muggli, E. Oz, R. H. Siemann, D. Walz, and M. Zhou, Nature **445**, 741 (2007).
[4] E. Kallos, T. Katsouleas, W. D. Kimura, K. Kusche, P. Muggli, I. Pavlishin, I. Pogorelsky, D. Stolyarov, and V. Yakimenko, Physical Review Letters **100**, 074802 (2008).
[5] AWAKE Collaboration, R. Assmann, R. Bingham, T. Bohl, C. Bracco, B. Buttenschön, A. Butterworth, A. Caldwell, S. Chattopadhyay, S. Cipiccia, E. Feldbaumer, R. A. Fonseca, B. Goddard, M. Gross, O. Grulke, E. Gschwendtner, J. Holloway, C. Huang, D. Jaroszynski, S. Jolly, P. Kempkes, N. Lopes, K. Lotov, J. Machacek, S. R. Mandry, J. W. McKenzie, M. Meddahi, B. L. Militsyn, N. Moschuering, P. Muggli, Z. Najmudin, T. C. Q. Noakes, P. A. Norreys, E. Öz, A. Pardons, A. Petrenko, A. Pukhov, K. Rieger, O. Reimann, H. Ruhl, E. Shaposhnikova, L. O. Silva, A. Sosedkin, R. Tarkeshian, R. M. G. N. Trines, T. Tückmantel, J. Vieira, H. Vincke, M. Wing, and G. Xia, Plasma Physics and Controlled Fusion **56**, 084013 (2014).
[6] T. Katsouleas, S. Wilks, P. Chen, J. M. Dawson, and J. J. Su, Particle Accelerators **22**, 81 (1987).
[7] W. Lu, C. Huang, M. Zhou, W. B. Mori, and T. Katsouleas, Physical Review Letters **96**, 165002 (2006).
[8] W. Lu, C. Huang, M. Zhou, M. Tzoufras, F. S. Tsung, W. B. Mori, and T. Katsouleas, Physics of Plasmas (1994-present) **13**, 056709 (2006).
[9] P. Muggli, B. Allen, Y. Fang, V. Yakimenko, M. Fedurin, K. Kusche, M. Babzien, C. Swinson, and R. Malone, in *Proceedings of PAC2011* (New York, NY, USA, 2011) pp. 712–714.
[10] A. Caldwell, K. Lotov, A. Pukhov, and F. Simon, Nature Physics **5**, 363 (2009).
[11] S. Steinke, J. van Tilborg, C. Benedetti, C. G. R. Geddes, C. B. Schroeder, J. Daniels, K. K. Swanson, A. J. Gonsalves, K. Nakamura, N. H. Matlis, B. H. Shaw, E. Esarey, and W. P. Leemans, Nature **530**, 190 (2016).
[12] C. A. Lindstrøm, E. Adli, J. M. Allen, J. P. Delahaye, M. J. Hogan, C. Joshi, P. Muggli, T. O. Raubenheimer, and V. Yakimenko, Nuclear Instruments and Methods in Physics Research Section A **829**, 224 (2016).
[13] E. Gschwendtner, E. Adli, L. Amorim, R. Apsimon, R. Assmann, A. M. Bachmann, F. Batsch, J. Bauche, V. K. Berglyd Olsen, M. Bernardini, R. Bingham, B. Biskup, T. Bohl, C. Bracco, P. N. Burrows, G. Burt, B. Buttenschön, A. Butterworth, A. Caldwell, M. Cas-

cella, E. Chevallay, S. Cipiccia, H. Damerau, L. Deacon, P. Dirksen, S. Doebert, U. Dorda, J. Farmer, V. Fedosseev, E. Feldbaumer, R. Fiorito, R. Fonseca, F. Friebel, A. A. Gorn, O. Grulke, J. Hansen, C. Hessler, W. Hofle, J. Holloway, M. Hüther, D. Jaroszynski, L. Jensen, S. Jolly, A. Joulaei, M. Kasim, F. Keeble, Y. Li, S. Liu, N. Lopes, K. V. Lotov, S. Mandry, R. Martorelli, M. Martyanov, S. Mazzoni, O. Mete, V. A. Minakov, J. Mitchell, J. Moody, P. Muggli, Z. Najmudin, P. Norreys, E. Öz, A. Pardons, K. Pepitone, A. Petrenko, G. Plyushchev, A. Pukhov, K. Rieger, H. Ruhl, F. Salveter, N. Savard, J. Schmidt, A. Seryi, E. Shaposhnikova, Z. M. Sheng, P. Sherwood, L. Silva, L. Soby, A. P. Sosedkin, R. I. Spitsyn, R. Trines, P. V. Tuev, M. Turner, V. Verzilov, J. Vieira, H. Vincke, Y. Wei, C. P. Welsch, M. Wing, G. Xia, and H. Zhang, Nuclear Instruments and Methods in Physics Research Section A **829**, 76 (2016).

[14] N. Kumar, A. Pukhov, and K. Lotov, Physical Review Letters **104**, 255003 (2010).

[15] E. Adli and AWAKE Collaboration, in *Proceedings of IPAC 2016*, International Particle Accelerator Conference (JACoW, Busan, Korea, 2016) pp. 2557–2560.

[16] V. K. Berglyd Olsen, E. Adli, P. Muggli, L. D. Amorim, and J. Vieira, in *Proceedings of IPAC 2015* (Richmond, VA, USA, 2015) pp. 2551–2554.

[17] R. A. Fonseca, L. O. Silva, F. S. Tsung, V. K. Decyk, W. Lu, C. Ren, W. B. Mori, S. Deng, S. Lee, T. Katsouleas, and J. C. Adam, in *Computational Science — ICCS 2002*, Lecture Notes in Computer Science No. 2331, edited by P. M. A. Sloot, A. G. Hoekstra, C. J. K. Tan, and J. J. Dongarra (Springer Berlin Heidelberg, 2002) pp. 342–351.

[18] V. K. Berglyd Olsen, E. Adli, P. Muggli, and J. Vieira, in *Proceedings of NAPAC 2016* (Chicago, IL, USA, 2016).

[19] C. Huang, V. K. Decyk, C. Ren, M. Zhou, W. Lu, W. B. Mori, J. H. Cooley, T. M. Antonsen, and T. Katsouleas, Journal of Computational Physics **217**, 658 (2006).

[20] W. An, V. K. Decyk, W. B. Mori, and T. M. Antonsen, Journal of Computational Physics **250**, 165 (2013).

[21] B. B. Godfrey, Journal of Computational Physics **15**, 504 (1974).

[22] R. Lehe, A. Lifschitz, C. Thaury, V. Malka, and X. Davoine, Physical Review Special Topics - Accelerators and Beams **16**, 021301 (2013).

[23] AWAKE Collaboration and A. Caldwell, *AWAKE Status Report, 2016*, Tech. Rep. CERN-SPSC-2016-033 (CERN, Geneva, 2016).

[24] M. Tzoufras, W. Lu, F. S. Tsung, C. Huang, W. B. Mori, T. Katsouleas, J. Vieira, R. A. Fonseca, and L. O. Silva, Physics of Plasmas **16**, 056705 (2009).

[25] J. B. Rosenzweig, G. Andonian, M. Ferrario, P. Muggli, O. Williams, V. Yakimenko, and K. Xuan, AIP Conference Proceedings **1299**, 500 (2010).

[26] J. B. Rosenzweig, B. Breizman, T. Katsouleas, and J. J. Su, Physical Review A **44**, R6189 (1991).